


6-2016

Influence of Low Temperature Degradation on Microstructural Integrity of Zirconia Dental Implants

Mona Monzavi Rahimi

Follow this and additional works at: <http://scholarsrepository.llu.edu/etd>

 Part of the [Dental Materials Commons](#), and the [Periodontics and Periodontology Commons](#)

Recommended Citation

Rahimi, Mona Monzavi, "Influence of Low Temperature Degradation on Microstructural Integrity of Zirconia Dental Implants" (2016). *Loma Linda University Electronic Theses, Dissertations & Projects*. 396.
<http://scholarsrepository.llu.edu/etd/396>

This Thesis is brought to you for free and open access by TheScholarsRepository@LLU: Digital Archive of Research, Scholarship & Creative Works. It has been accepted for inclusion in Loma Linda University Electronic Theses, Dissertations & Projects by an authorized administrator of TheScholarsRepository@LLU: Digital Archive of Research, Scholarship & Creative Works. For more information, please contact scholarsrepository@llu.edu.

LOMA LINDA UNIVERSITY
School of Dentistry
In conjunction with the
Faculty of Graduate Studies

Influence of Low Temperature Degradation on Microstructural Integrity of Zirconia
Dental Implants

by

Mona Monzavi Rahimi

A Thesis submitted in partial satisfaction of
the requirements for the degree
Master of Science in Periodontics

June 2016

© 2016

Mona Monzavi Rahimi
All Rights Reserved

Each person whose signature appears below certifies that this thesis in his/her opinion is adequate, in scope and quality, as a thesis for the degree Masters of Science.

_____, Chairperson
Erik Sahl, Assistant Professor of Periodontics

Tord Lundgren, Professor of Periodontics

Rodrigo Viecilli, Associate Professor of Orthodontics and Dentofacial Orthopedics

ACKNOWLEDGEMENTS

I would like to thank the member of my committee for their leadership and direction, Dr. Stefan Kraemer for providing guidance on my microscopy analysis, Dr. Sammy Noubissi for his advice and support throughout the study, Dr. Yoon Jeong Kim and Dr. Dennis Smith for reviewing, editing and making valuable comments for my protocol and manuscript, Dr. Oyoyo for statistical analysis and company Z-system company and Straumann for donating implants for this research project. At last I would like to thank my family for their everlasting love and support.

CONTENT

Approval Page.....	iii
Acknowledgements.....	iv
Table of Contents.....	v-vi
List of Figures.....	vii
List of Tables.....	viii
List of Abbreviations.....	ix
Abstract.....	x
Chapter	
1. Introduction and Literature Review.....	1
Zirconia Microstructural Properties.....	1
Stressed-induced Transformation Toughening.....	2
Low Temperature Degradation (LTD).....	3
LTD Related Problems of Bio-ceramics.....	4
Current Techniques for Assessing LTD.....	7
Study Aim.....	8
2. Materials and Methods.....	9
Implant Description.....	9
Accelerated Aging Test.....	12
FIB/SEM Investigation.....	13
Statistical Analysis.....	15
3. Results.....	17
Microstructural Features of “As received Implants”- SEM analysis.....	17
Microstructural Features of “As received Implants”- FIB analysis.....	24
Microstructural features of aged implants.....	29
Statistical results.....	31
4. Discussion.....	37
5. Conclusions and Future Directions.....	41

References.....42

FIGURES

Figures	Page
1. Scheme for Stress Induced Transformation Toughening.....	3
2. Type A Implants Processing Information.....	10
3. Sample Preparation.....	14
4. FIB/SEM System.....	15
5. Type A Surface SEM.....	18
6. Type B Surface SEM.....	19-20
7. Type C Surface SEM.....	21-22
8. Type D Surface SEM.....	23-24
9. FIB Ionic Sectioning.....	26
10. FIB Cross Sections of As-received Implants.....	27-28
11. FIB Cross Sections of Aged Implants.....	31

TABLES

Tables	Page
1. Type A composition and properties	11
2. Spearman's rho correlation	33
3. Kruskal-Wallis Test: Micro-crack formation.....	33
4. Kruskal-Wallis Test: T-M Transformation	34
5. Dunn Bonferroni Pairwise Comparison Prior to Aging.....	35
6. Dunn Bonferroni Pairwise Comparison at 30 Hours	36

ABBREVIATIONS

Zr ₄₀	Zirconium
ZrSiO ₄	Zircon/Jargon (Zirconium orthosilicate)
ZrO ₂	Zirconia
Y-TZP	Yttrium Stabilized Tetragonal Zirconia Polycrystal
LTD	Low Temperature Degradation
MgO	Magnesium Oxide
CaO	Calcium Oxide
Y ₂ O ₃	Yttrium Oxide
CeO ₂	Cerium Oxide
Al ₂ O ₃ -YSZ	Alumina-zirconia composites
ATZ	Alumina toughened zirconia

ABSTRACT OF THE THESIS

Influence of Low Temperature Degradation on Microstructural Integrity of Zirconia Dental Implants

By

Mona Monzavi Rahimi

Master of Science, Advanced Specialty Education in Periodontics and Implant Surgery
Loma Linda University, March 2016
Dr. Erik Sahl, Chairperson

Zirconia dental implants have become more popular in the field of implant dentistry. However, concerns have been raised regarding low temperature degradation and its influence on phase stability and micro-structural integrity in terms of increased micro-crack formation. In the case of dental implants, this could possibly result in delamination and interference with bone to implant contact and eventually lead to loss of integration and failure. Nevertheless, no study has reported the effects on commercially available Zirconia dental implants.

The primary aims of this study was to determine if there is a correlation between ageing duration and 1) depth of tetragonal-monoclinic phase transformation (t-m transformation), 2) micro-crack formation of commercially available Zirconia dental implants. A secondary aim was to compare the depth of t-m transformation, micro-crack formation as the result of ageing between different commercially available Zirconia dental implants.

Accelerated aging at increased temperature, moisture and pressure were performed using an autoclave technique to artificially age Zirconia dental implants. There were a total of 36 implants from four companies, three of which were commercially

available. Each group had nine implants, with three samples evaluated prior to aging and three at 15 and 30 hours of aging. Focused ion beam-scanning electron microscopy analysis was performed to determine the microstructural features of the surface and bulk of as-received implants and to investigate the aging effect on microstructural integrity defined by the t-m transformation and formation of micro-cracks on the aged implants.

Pre-existing grain transformation around surface porosities and micro-cracks were most evident in types A, B, C and were significantly higher in A compared to C ($p \leq 0.05$). No significant differences were found among groups at 15 hours. At 30 hours, the depth of the t-m transformation and quantity of micro-cracks increased for A, C and D and a significantly higher transformation was found for type A compared to type B ($p \leq 0.05$). Type B microstructure seemed to be least affected by LTD at 30 hours. A strong correlation between ageing duration and depth of t-m transformation at 15 and 30 hours was found ($p \leq 0.01$) for all implants combined.

Within the limitations of this study we concluded that aging led to loss in microstructural integrity described by transformation of grains and increased number of porosities and microcracks for types A, C and D, a finding most apparent at 30 hours. The effect of aging on microstructural integrity is likely more related to composition and structural details of implants, than their surface treatment.

CHAPTER ONE

INTRODUCTION AND LITERATURE REVIEW

Zirconia Microstructural Properties

The name of the metal Zirconium is taken from the mineral name Zircon, which comes from a Persian word Zargun meaning gold colored. Zirconia, the metal dioxide (ZrO_2) was discovered from Zircon in 1789 by the German chemist Martin Heinrich Klaproth and it was mainly used in combination with various earth oxides as a pigment for ceramics [1].

Pure Zirconia oxide is a polymorph that exists in three distinctive crystal phases at different temperatures [2]. At room temperature it exists in a monoclinic phase (largest), but transforms into a tetragonal phase (smallest) above 1170°C and at 2370°C it becomes cubic (intermediate) [2]. During cooling, a T-M transformation takes place in a temperature range of about 100°C below 1070°C . The phase transformations at the time of cooling are accompanied by a substantial volume increase of approximately 4.5% and thus shear strain. Stresses produced by the volume expansion originate cracks in pure zirconia ceramics that, after sintering in the range of $1500\text{-}1700^\circ\text{C}$, it breaks into pieces at room temperature leading to catastrophic failure [3,4]. Consequently, this enormous volume expansion prevented use of Zirconia as a bulk material. Nevertheless, later an important discovery revealed that the tetragonal, or even the cubic form could be retained metastably at room temperatures by alloying zirconia with other stabilizing oxides such as CaO, MgO, Y_2O_3 , CeO_2 , Er_2O_3 , Eu_2O_3 , Gd_2O_3 , Sc_2O_3 , La_2O_3 and Yb_2O_3 , thus preventing the catastrophic failure of pure zirconia [5,6]. Currently, the most studied stabilizers for biomaterials applications are CaO [7], MgO [8], Y_2O_3 [9], and CeO_2 [10],

and of these stabilizers, yttria (Y_2O_3) is the most frequently used for dental applications. When stabilized with approximately 3 mol% yttria, zirconia is composed of metastable tetragonal phase. This type of material is referred to as yttria-stabilized tetragonal zirconia polycrystals (3Y-TZP), which can be used as a bulk material [11].

Stressed-induced Transformation Toughening

In the mid to late 1970's, it was further revealed that the t-m transformation with its subsequent volume expansion could be used to enhance the fracture toughness of Zirconia-based materials. This led to discovery that the metastable Zirconia displays a stress-induced transformation toughening mechanism, which resists crack propagation [12, 13]. This mechanism involves transformation of a metastable tetragonal to monoclinic phase during mechanical stress. Since the phase transformation is accompanied by the volume expansion of grains, compressive stress is generated in localized areas around micro-cracks, resulting in arrested crack propagation [12, 13]. Therefore, these metastable tetragonal ceramics demonstrate remarkable toughness when the transformation to monoclinic phase is triggered by a propagating crack [14]. In Fig 1 a schematic illustration of this phenomenon is shown.

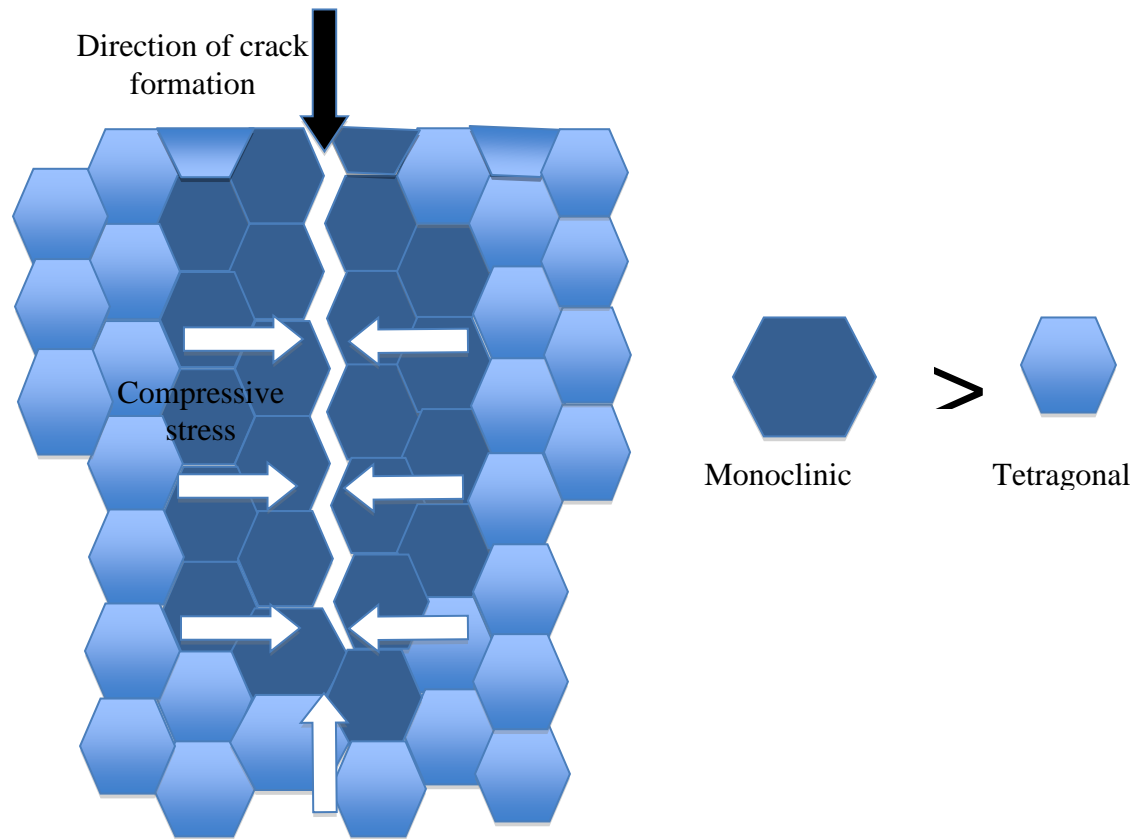


Figure 1. Schematic presentation of stress-induced transformation toughening phenomenon of Y-TZP. The figure is modified from (Picconi and Maccauro, 1999)

This discovery led to the development of high toughness ceramics namely Yttria-stabilized Tetragonal Zirconia Polycrystal (Y-TZP), in order to stabilize the tetragonal phase at room temperature [14]. These metastable tetragonal ceramics demonstrate remarkable toughness when the transformation to monoclinic phase is triggered by a propagating crack [14].

Low Temperature Degradation (LTD)

It was later revealed that in presence of moisture and lack of mechanical stress the

metastable tetragonal phase in Y-TZP suffers a spontaneous tetragonal-monoclinic phase transformation (t-m transformation) at the sample surface, which continues to the bulk of the material. This process occurs at much lower temperatures (65° C-300 °C) than it normally occurs (1000 ° C) and was referred to as “ageing” or “LTD” [15].

Transformation first occurs at a specific grain on the surface that is more susceptible to the phase transformation because of a disequilibrium state, which may include lower content of stabilizer, presence of residual stress or a large grain size [16]. Since the transformation is accompanied by volume expansion of crystalline structure, it causes surface uplift and micro cracks, leading to surface roughening and grain delamination. The formation of micro cracks then allows water to penetrate below the surface, thus propagating the t-m transformation to the interior of the sample [17]. Finally, it leads to development of major cracks and failure of the material [18].

Despite numerous attempts, the exact mechanism of slow t-m transformation triggered by water molecules is still under question [19]. Nonetheless following steps have been proposed [20, 21, 22]:

- Chemical adsorption of H₂O on ZrO₂ surfaces
- Formation of Zr-OH bond disrupting Zr-O-Zr bond
- Penetration of OH⁻ and/or O²⁻ into the inner part by grain boundary diffusion
- Filling of oxygen vacancies by OH⁻ and/O²⁻
- Reduction of the oxygen vacancies destabilizing tetragonal phase

LTD Related Problems of Bio-ceramics

The problem of LTD in zirconia (Y-TZP) was first reported in an in vitro study in

1981 [15] and along with other studies it was found that LTD progresses most rapidly at temperatures of 200-300 °C. Hence its effect on zirconia biomaterials was considered to be negligible at body temperature (37 ° C) [21, 23] and in the late 1980's, Y-TZP gained popularity for the manufacture of femoral heads for hip prosthesis application [24]. Nevertheless, in 2001 a series of Zirconia femoral head failures were reported as a result of LTD, and its usage in orthopedics was terminated [19] with major companies switching to two phased alumina-zirconia composites (Al_2O_3 -YSZ) [22]. To present, the influence of LTD on prosthetic femoral heads has been well studied for many years and has demonstrated a progressive increase in surface roughness, delamination/grain pullout and eventually fracture, due to extension of micro-cracks and generation of large cracks [19, 25]. The kinetics of LTD is thought to be highly dependent on the processing conditions and the resulting microstructure of the material. For instance, it is widely accepted that large grain size as a result of high sintering temperatures generally triggers transformation. Similarly, low density and open porosities due to incomplete sintering allow water to diffuse towards greater depth and increase susceptibility to LTD [19, 22]. In terms of dental applications, LTD is a relatively new subject with only few studies available. Nevertheless, due to its superior esthetic properties, biocompatibility, mechanical properties, and low plaque affinity, Y-TZP has gained greater popularity in dental applications, including dental implants, and restorative prostheses [26, 27, 28]. However, review articles have emphasized that long-term investigations are greatly needed to properly evaluate Zirconia for clinical application [26, 29]. Current research on zirconia dental ceramics have focused on their mechanical properties [30], fatigue resistance [31], and surface modification to enhance bone in-growth [32].

The investigation for better implant osseointegration has led researchers to develop methods to increase surface roughness and/or microporosity. Though surface modifications may improve bone in-growth, it could also trigger t-m transformation with associated volume increase leading to formation of surface compressive stress thereby altering the phase integrity of the material and increasing the susceptibility to aging [11]. One is reminded that Zirconia (Y-TZP) in dental applications can be expected to be as susceptible to LTD as orthopedic applications with exhibiting the same dependency against process variation [22, 27].

Recent in vitro studies have concluded that Y-TZP dental ceramic is susceptible to LTD, which results in increased surface roughness [33, 34], and micro-cracking in the bulk [35] or both bulk and porous coating [27]. The practical consequences of such extensive micro-cracking in terms of dental implants may be exfoliation of the surface porous layer and delamination from the bulk, which may further result in loss of integration [27]. Therefore, it was advocated that generalizations must be avoided when considering aging of zirconia dental products and that every new material/process combination should be tested before drawing conclusions [35, 27]

In terms of the effects of LTD on the strength of Zirconia, the results are quite variable. A review article on orthopedic implants revealed that strength of Zirconia could decrease or increase by aging with time [1]. Other studies revealed a reduction in Young's modulus and hardness [33, 36], and reduction of flexural strength [37]. Further recent studies demonstrated that a considerable degree of t-m transformation did not lead to a decrease in strength [38] or even led to a significant increase in strength [35, 27, 39]. Regardless of available contradictory results on strength, its verified influence on

structural integrity in terms of micro-cracking and increased surface roughness may influence its interaction with surrounding bone and soft tissue. Therefore, it is important to accurately characterize the effect of LTD on surface coating and bulk of dental implants.

Current Techniques to Evaluate Influence of LTD

X-ray diffraction (XRD) technique has long been a common approach for evaluation of t-m transformation following LTD. A recent study evaluated the t-m transformation following accelerated ageing, utilizing Focused Ion Beam (FIB)-Scanning Electron Microscopy (SEM) experiments in addition to XRD technique [35]. Results revealed that XRD was unable to properly characterize the transformation rate features throughout the bulk of the implant below its coating as it only penetrates between 5-15 microns, with coating thickness being 10-15 microns. Focused Ion Beam (FIB) experiments showed that the t-m transformation did not occur in the coating but initiated at the interface of coating to bulk. This finding revealed that XRD data would result in a high underestimation of the transformation in the bulk material. Therefore, if it is utilized alone as in most studies, XRD can result in incorrect data, which can be misleading for clinical applications. This study urged the use of FIB/SEM instruments to enable precise investigation of the t-m transformation [35].

Currently available zirconia dental implant systems have considerable differences with regards to their surface preparation and processing [26]. These existing differences may influence their vulnerability or resistance to aging. The search for improved osseointegration has led to emergence of methods to increase surface roughness and

micro-porosities. Increased surface roughness may positively influence bone apposition and in-growth, but could also facilitate water penetration into the bulk and lead to modification of tetragonal phase under humid atmosphere and thus facilitate aging [35]. Previous studies have indicated that the low temperature degradation of every new surface modification should be carefully evaluated. Generalizations may be avoided by testing all new material/process combinations, before drawing conclusions. Any modification in the process could dramatically change the LTD resistance [27, 35].

Study Aim

There are currently no studies, which have attempted to compare the effects of LTD on these commercially available dental implant systems, considering their differences in surface treatment, bulk composition and micro-structure. The available studies are concerned with medical grade Zirconia and have been performed on bending bars or discs, which are polished and therefore not relevant for dental implants. A recent investigation has proposed a protocol to validate the functionality and safety of Zirconia dental implants prior to their clinical use [40]. To our knowledge, this present study will be the first to utilize this protocol to evaluate the effect of LTD on micro-structural properties of four commercially available Zirconia dental implant systems. Therefore, the primary aim of the present study is to assess the effect of ageing on microstructure of commercially available Zirconia dental implants in terms of extent of phase transformation and micro-crack formation. The secondary aim is to compare the micro-structural changes between these four groups as a result of ageing.

CHAPTER TWO

MATERIALS AND METHODS

LTD of four types of Y-TZP implant systems were examined and compared via:

- Accelerated aging test conducted for 15 and 30 hours at 134 °C and 2-bar pressure
- FIB-SEM analysis to obtain 3 dimensional (3D) insights into the micro-structural features of the surface and the bulk on 12 as-received implants (n=3 per group), and in-depth effects of ageing on 24 aged implants (n=6 per group).

Implant Description

Four different types of zirconia dental implants were investigated (Type A, Type B, Type C, and Type D; 9 implants, respectively). Amongst these implants type A, B and C are commercially available and type D was discontinued in 2010 due to increased fracture. In each group (n=9 per group) three implants were examined prior to aging, followed by three implants at 10 hours of aging and three implants at nine hours of aging.

Type A implants (Z systems®, Z5c Zircolith®, Basel) comprised of Z-system Full Ceram implants made from ZrO₂ TZP-A HIP bio-ceramics according to ISO 13356. Implants had a screw design shape with a tapering thread and widened core diameter in the upper part of the thread. Implants had a shoulder diameter of 6.0mm, outer diameter of 5mm and length of 12mm. The surface of type B implants has been sand blasted and laser-modified with a patented laser process. The material composition and processing of type A implants are described in Figure 1 and Table 1 respectively.

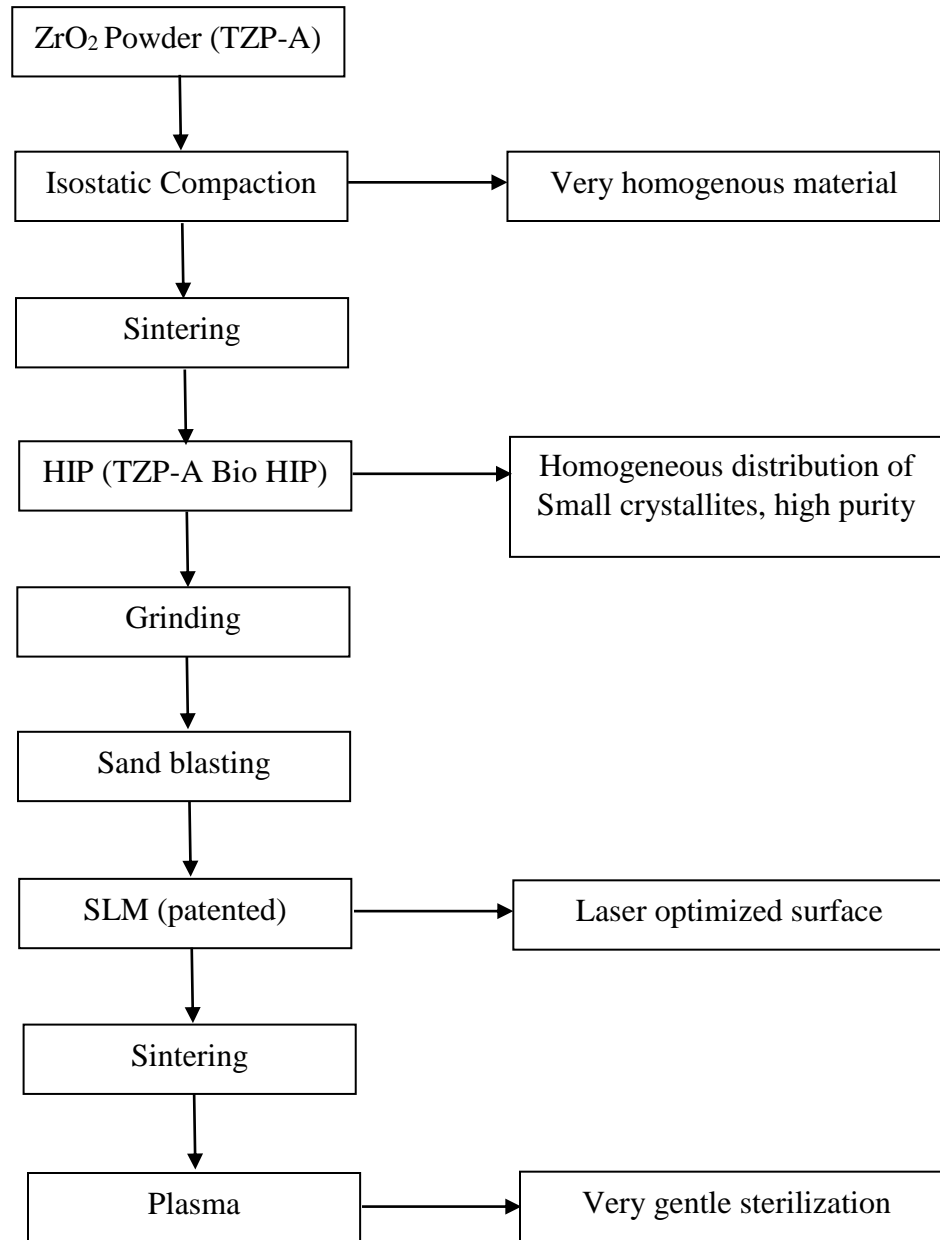


Fig 2. Type A processing information

Table 1. Information on properties and material composition of type A implants

Designation		TZP	TZP-A	FSZ	PSZ	ATZ
Components		ZrO ₂ /Y ₂ O ₃	ZrO ₂ /Y ₂ O ₃ /Al ₂ O ₃	ZrO ₂ /Y ₂ O ₃	ZrO ₂ /MgO	ZrO ₂ /Al ₂ O ₃ /Y ₂ O ₃
Composition	%	95/5	95/5/0.25	90/10	96.5/3.5	76/20/4
Density	g/cm ³	6.05	6.05	5.8	5.7	5.5
Open porosity	%	0	0	0	0	0
Grain size (mli)	µm	0.4	0.35	10	20	0.4
Hardness Vickers	Hv	1200	1200	1200	1500	1400
Hardness Mohs		8	8	8	>8	8
Compressive strength	MPa	2000	2000	2000	2000	2000
Flexural strength	MPa	1000	1200	250	500	2000
Young's modulus	GPa	200	210	150	200	220
Fracture toughness K _{1c}	MN/m ^{3/2}	8	8	-	10	8
Poisson ratio	-	0.31	0.31	-	0.23	0.3
Max. operating temperature	°C	1000	1000	2000	1000	1000
Thermal expansion (20-1000°C)	10 ⁻⁶ /K	10	10	10	10	9
Thermal conductivity	W/mK	2.5	2.5	2.5	2	6
Specific heat	J/kg K	500	500	500	550	600
Dielectric strength	kV/mm	-	-	-	-	-
Electrical resistivity (20 °C/1000 °C)	_ cm	-	-	-	10 ¹⁵ /3.0	-
Dielectric constant (100 MHz)	_	-	-	-	-	-
Dielectric loss factor	tan _	-	-	-	-	-
Shaping procedures:						
Isostatic pressing		X	X	X	X	X
Die pressing		X	X		X	X
Slip casting				X		
HIP		X	X			X
Suggested applications		Bioceramic, Precision parts	Bioceramic (Orthopaedics, Dental), Precision parts	Probes, Crucibles, Tubes	Tubes, Plates, Precision parts	Bioceramic (Orthopaedics, Dental), heavy-duty wear-resistant parts

Type B implants (Straumann® Pure Ceramic Implant, Basel) were monotype Straumann Full Ceram implants made from yttria-stabilized zirconia (in accordance with ISO 13356). The implants consisted of a tissue level platform with a 1.8 mm transmucosal neck, a 4.8 mm shoulder diameter, an abutment as an inherent part of the implant body and a cylindrical endosseous part with a screw design and a coronal tapered thread core diameter (known from Straumann Bone Level implants). The outer diameter

including the threads was 4.1 mm, the thread pitch 0.8 mm, the abutment height 4mm and the total endosseous length 12 mm. From the limited information provided from the manufacturer, the processing of Type B implants consisted of powder preparation, spray drying, cylinder pressing, sintering, HIP, machining, with sand blasting and etching of the surface.

Type C implants (Ceraroot®, Barcelona) were Ceraroot Full Ceram implants made from yttria-stabilized zirconia: ZrO_2 (95%) + Y_2O_3 (3%). The ceramic raw material was first pressed and molded into cylinders then pre sintered and machined to final shape with CAD/CAM, and finally sintered to full density [41]. The surface of type C implants had an acid etched ICE surface® topography. Implants consisted of one-piece tissue level implant in different lengths and diameters.

Type D implants (Zeramex® Dental point, Zurich) a full ceramic implant system made from Yttria-stabilized zirconia, ZrO_2/Y_2O_3 (95/5). Surface of implants were sandblasted with Al_2O_3 and acid etched with H_3PO_2 [42]. Implants consisted of combination of one-piece and two-piece in different lengths and diameters. According to the manufacturer these implants were discontinued in 2010 due to increased fracture rate and replaced with alumina toughened zirconia (ATZ).

Accelerated Aging Test

Aging kinetics was evaluated by performing accelerated aging tests on a series of 36 implants (six from each company) in water steam at 134°C, under two bar pressure for 15 and 30 hours (n=3 at each interval). It has been reported that one hour at 134°C would approximately correspond to two years at body temperature (37°C) under no pressure.

This is a rough estimation that can be debated but gives an idea of treatment durations pertinent for the application [23]. Moreover, effects of aging were specially examined after zero, 15 and 30 hours of artificial aging (n=3 per interval), because this aging duration approximately represents the range of the lifetime expected for endosseous implants corresponding to 30 years and above in vivo [23]. A new set of implants was examined at each interval, as examining the same area each time could have resulted in more extensive phase transformation and micro-cracking and biased result.

FIB-SEM Investigation

FIB-SEM experiments were performed on non aged followed by aged implants, to obtain insights into the microstructural features from the surface to the bulk and to follow in depth the effects of aging on t-m transformation and micro-crack formation. A fixation mount was fabricated for different sizes of dental implants. Dental implants were fixated with copper tape and portion of their surface were coated with platinum gold to provide surface conductivity. Samples were rotated to have the threads along the y-axis as shown in Figure. 2. SEM images made from the surface at different magnifications. FIB cross-sectional scans were made specifically at the crest of the second thread to investigate the endo-osseous portion of the implant. FIB imaging was performed using FIB (FEI™ DB235 Dual-Beam™, Eindhoven) w/ Energy Dispersive X-ray Spectroscopy (EDAX® EDS, Mahwah). A Schottkey emitter™(FEI™, Thermal Field Emitter, Eindhoven) was used for SEM under 200-300 kV, whereas Gallium liquid metal was used for focus ion beam (FIB) operated at 5 to 30 kV. The resolution was 3 nm for SEM and 7 nm for FIB. In brief, the FIB used a liquid metal ion source of Ga⁺ ions accelerated between two and

30 KeV that were focused to the surface to cut slices of materials. SEM images were then taken from the cross sectional slice. FIB/SEM analysis therefore produced images from the cross sectional slices from the bulk of dental implants. Analysis was made in TLD immersion mode, secondary electron, imaging 9.7 pA, digging 9.3 pA, 5 Kv surface cleaning. Depth of t-m transformation and micro-crack formation were measured for each implant and averaged for each implant group (N=3) at 0, 15, 30 hours.

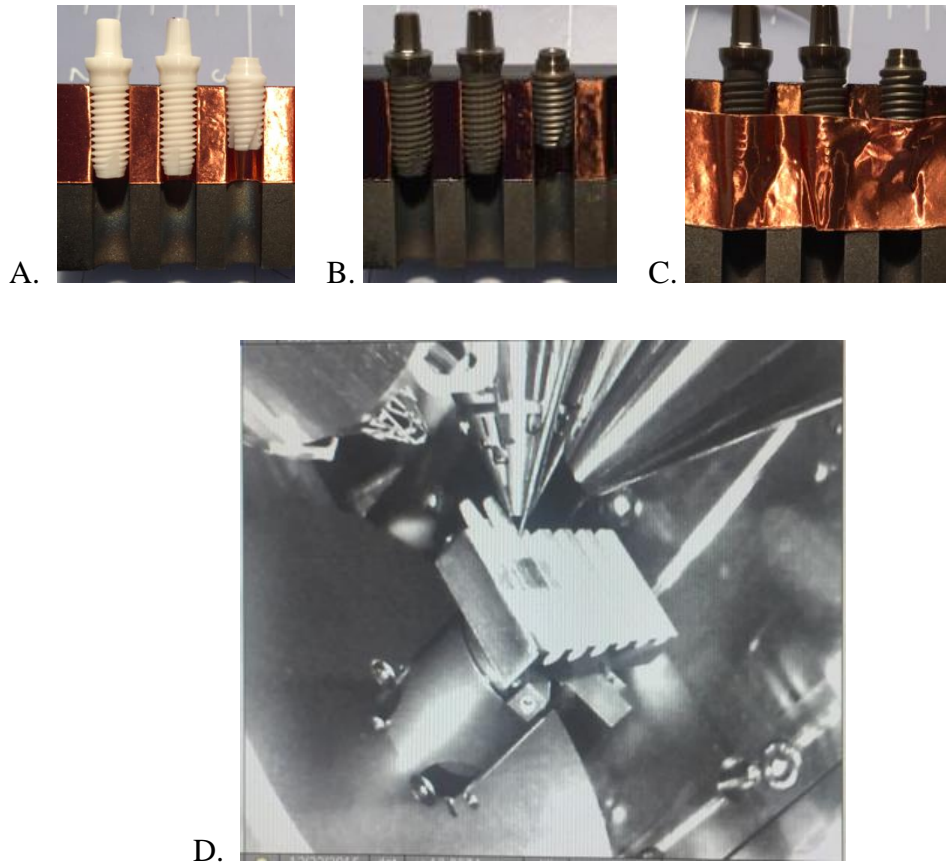


Figure. 3. A. Implants prior to coating, B. Implants coated with platinum gold, C. Coated implants fixated with lead tape. D. Samples rotated to have the threads along the Y-axis

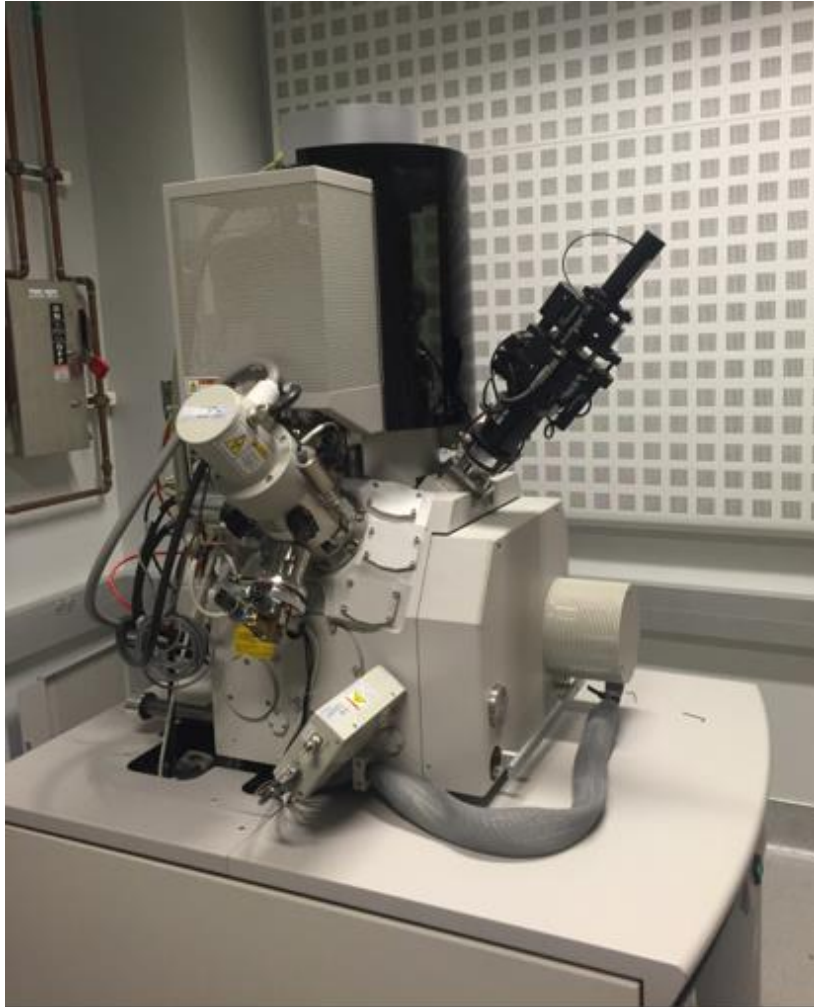


Fig. 4. FEI DB235 Dual-Beam Focus Ion Beam System (FIB) with EDS

Statistical Analysis

Longest depth of micro-crack formation and t-m transformation were measured and averaged for different time points within each group. The sample size was based on past publications and resources [24]. Small sample size and lack of normality warranted the use of non-parametric Spearman's rho correlation coefficient to evaluate the correlation between duration of aging and depth of t-m transformation and micro-crack formation. Independent sample Kruskal-Wallis test was performed to determine

significant differences between groups. Dunn Bonferroni Pairwise comparison analysis was completed at different time points to determine differences between groups. Hypotheses related to each predictor were tested at an alpha level of 0.05 and 95% confidence interval were constructed around each beta coefficient. All analysis was performed using SPSS 23 V (SPSS Inc, Chicago, IL).

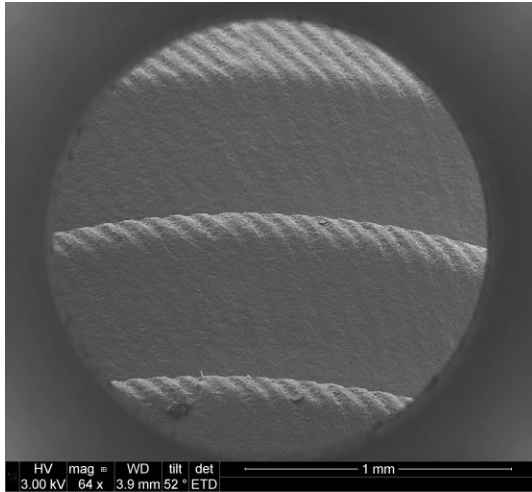
CHAPTER THREE

RESULTS

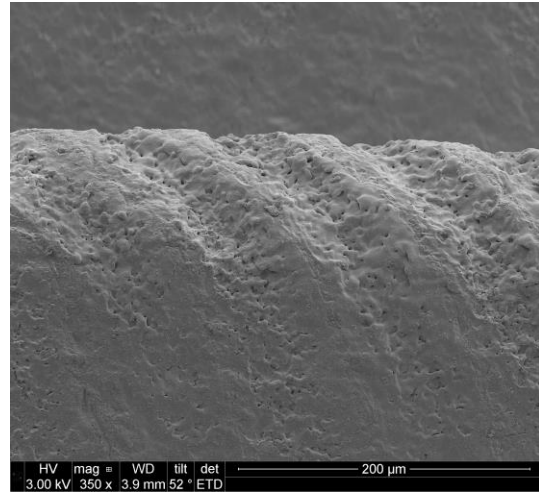
Microstructural Features of “As-received Implants”- SEM analysis

SEM images of the 4 types of implants and their typical surface features are given in Figure. 4-7, at different magnifications. High magnification images have been taken from crest of the second thread.

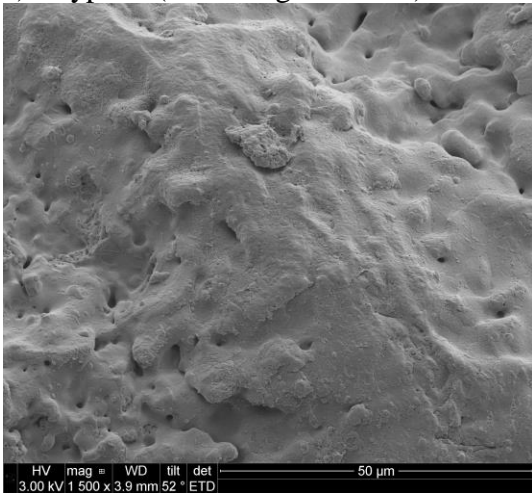
Type A implants exhibits a v-shaped thread design with rounded edges and symmetrical sides inclined at equal angle. SLM[®] (surface laser modified) procedure was completed only on the crest and flanks of the thread. Laser modified roughened surfaces had a melting structure characterized by symmetrical parallel grooves at the crest of the threads. High magnification showed few micro-cracks and micro-porous surface structure with pore size ranging from 0.3 to 5 μm .



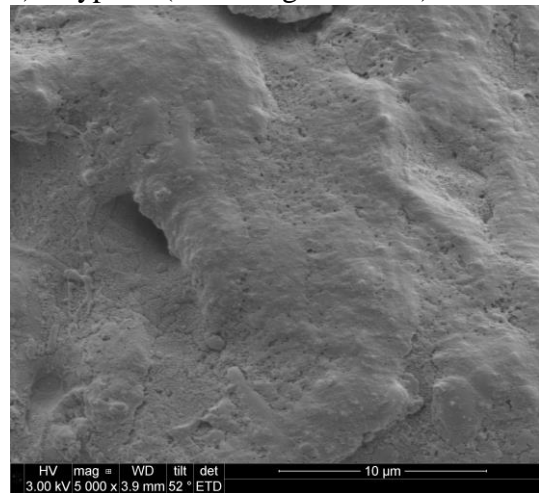
a) Type A (Low Magnification)



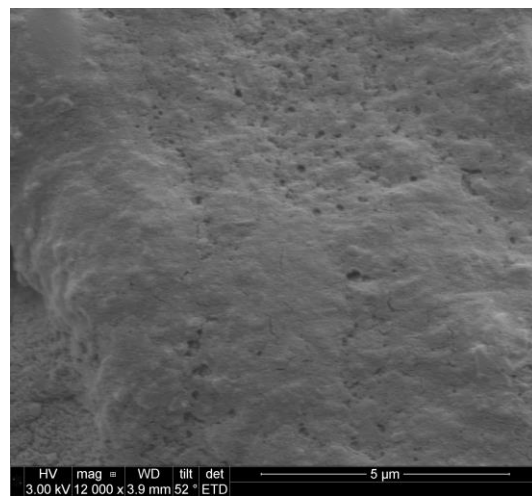
b) Type A (Low Magnification)



c) Type A- High Magnification (50 μm)



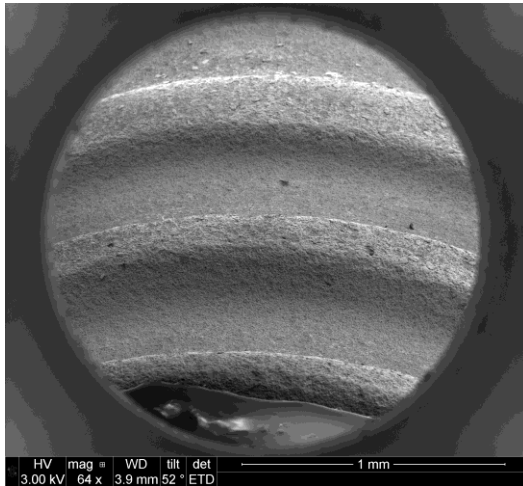
d) Type A- High Magnification (10 μm)



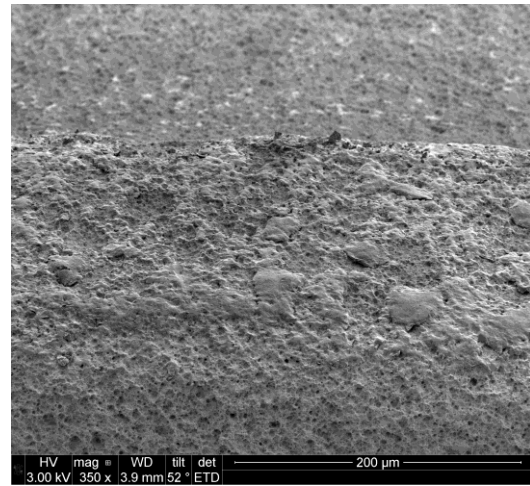
e) Type A. High Magnification (5 μm)

Figure. 5 - SEM images of type A (Z systems®, Z5c Zircolith®, Basel) from lowest to highest magnification.

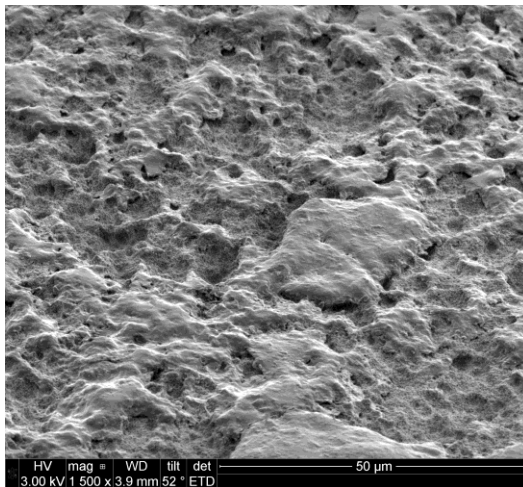
Type B implants with sand blasted and an acid etched surface had a buttress-shaped thread design with sharp square edges and non-symmetrical sides. High magnification showed numerous micro pits with sharp and rounded edges. Micro-pores were visible with in pits and over flat surfaces.



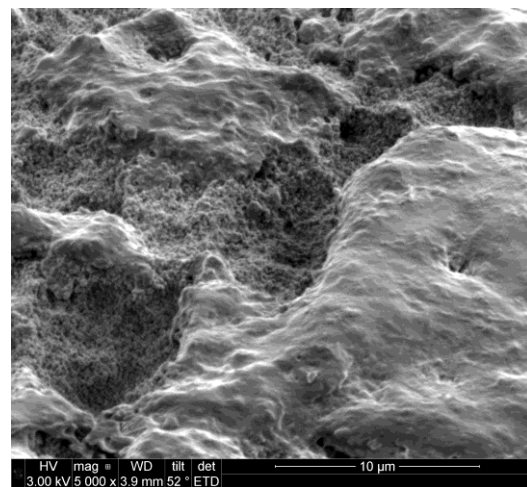
a) Type B. Low Magnification



b) Type B. Low Magnification (200 µm)

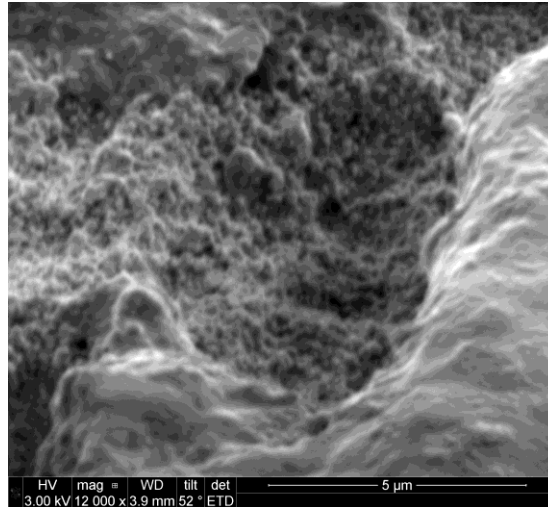


b) Type B. High Magnification (50 µm)



c) Type B. High Magnification (10 µm)

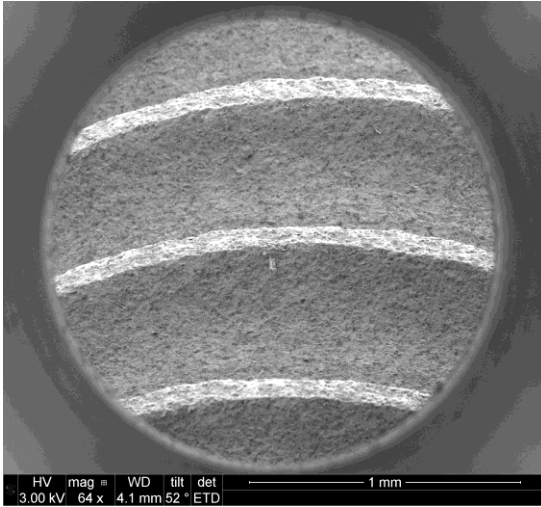
Figure. 6- SEM images of type B implants (Straumann® Pure Ceramic Implant, Basel)



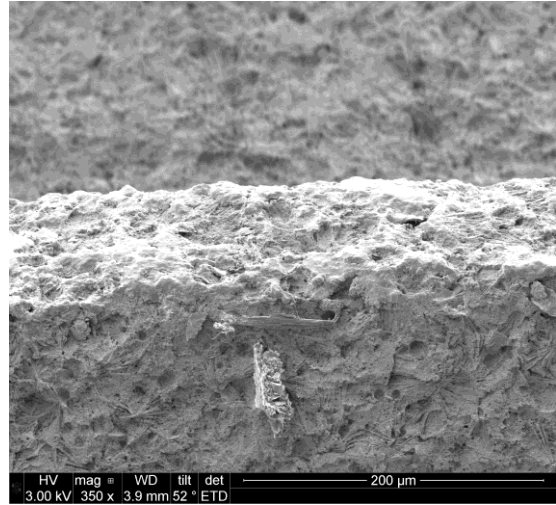
d) Type B. High Magnification (5 μm)

Figure. 6- (*Continued*) SEM images of type B implants (Straumann® Pure Ceramic Implant, Basel)

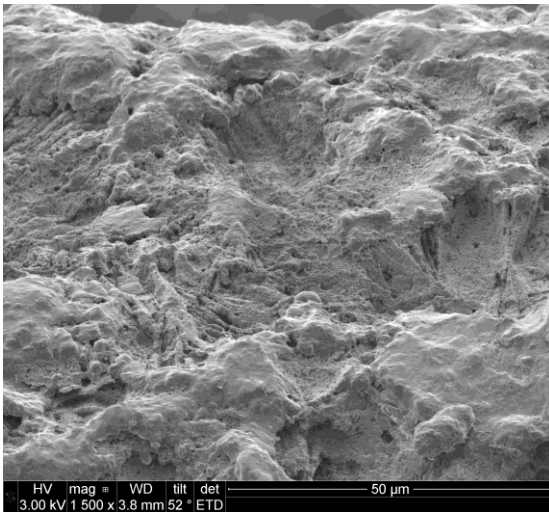
Type C implants with acid etched surface had a square shaped thread design with symmetrical sides perpendicular to the axis of the screw head. Low magnification images showed repeating patterns of multiple grooves with a divergent design forming half or full circles. High magnification showed a very prominent heterogeneous surface topography consisting of combination of grooves, pits and micro-pores.



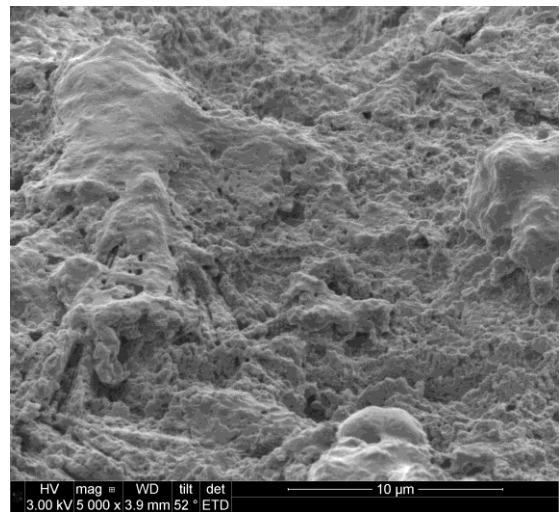
a) Type C- Low Magnification



b) Type C- Low Magnification (200 μm)

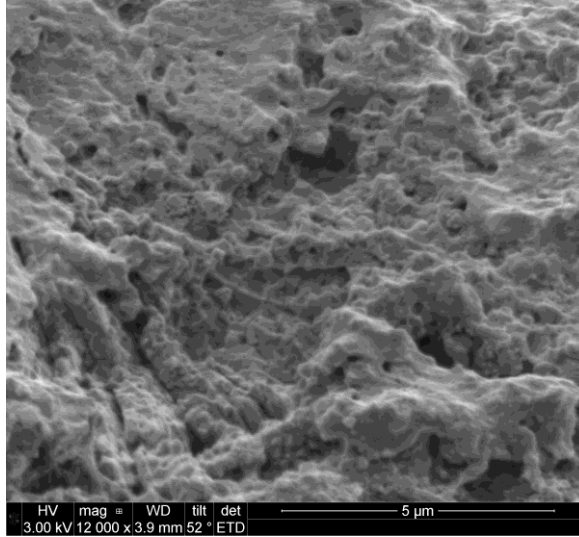


c) Type C- High Magnification (50 μm)



d) Type C- High Magnification (10 μm)

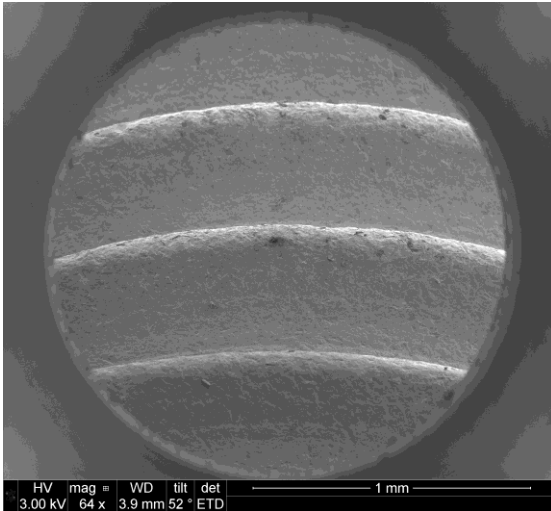
Figure. 7- SEM images of as received type C implant (Ceraroot®, Barcelona) from lowest to highest magnification



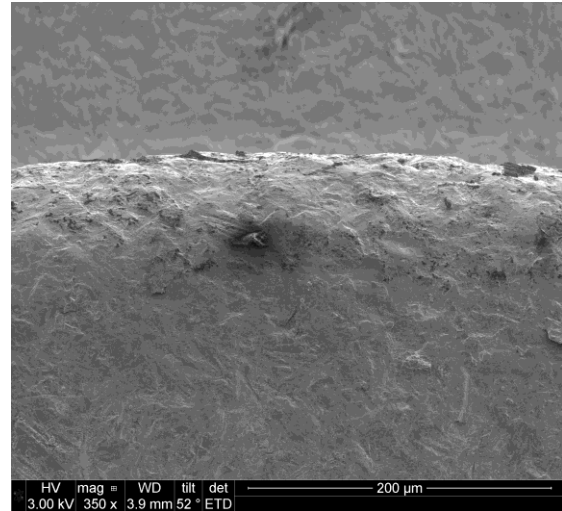
Type C- High Magnification (5 μm)

Figure. 7- (Continued) SEM images of as received type C implant (Ceraroot®, Barcelona) from lowest to highest magnification

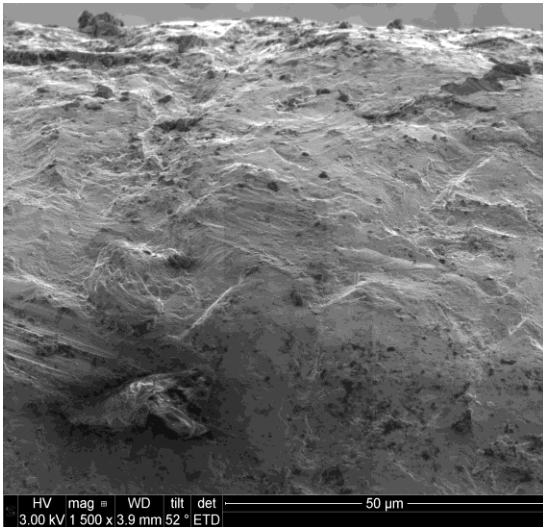
Type D implants exhibited a v-shaped thread design with flat, curved edges and symmetrical sides inclined at equal angle. The SEM image of the sand blasted and acid etched surface showed relatively smoother surface compared to the last three implant types. Surface roughness consisted of a regular pattern of shallow grooves with few micro-cracks. Aluminum-rich particles were seen on the surface resulting from the blasting process.



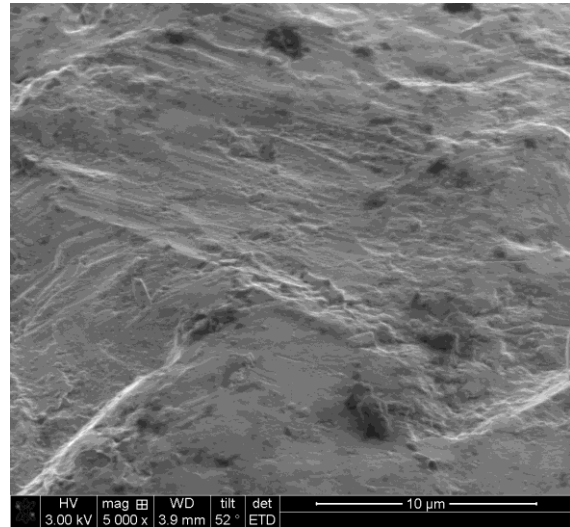
a) Type D- Low Magnification



b) Type D- Low Magnification

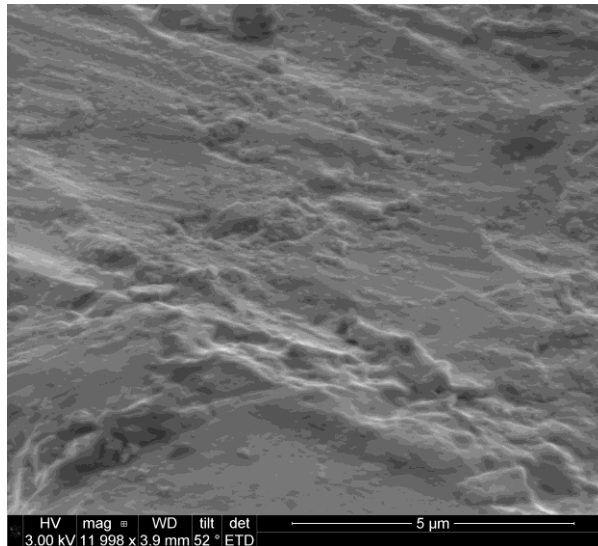


b) Type D- High Magnification (50 μm)



c) Type D- High Magnification (10 μm)

Figure. 8- SEM images of as received type D implant (Zeramex® Dental point, Zurich) from lowest to highest magnification



d) Type D- High Magnification (5 μm)

Figure. 8- (*Continued*) SEM images of as received type D implant (Zeramex® Dental point, Zurich) from lowest to highest magnification

Microstructural Features of “As-received Implants”- FIB analysis

Cross sectional (FIB) images were taken from 12 implants in four groups (n=3).

Figure 2 provides a low magnification image, demonstrating the location of ionic sectioning of implant at the crest of second thread. High magnification images of FIB slices for each implant are shown in Figure 3. Transformation of grains from tetragonal to monoclinic phase was determined by a modified contrast with presence of twining or loss of grain boundaries.

Type A implant presented with pre-existing surface porosities and micro-cracks, which extended an average depth of 0.5 μm , also observed on surface SEM images. Surface micro-pores were interconnected in few areas, which could allow access for fluid to enter the bulk during accelerated aging procedure. Zirconia grains showed evidence of

twining around cracks and pores, which expanded an average distance of 2.6 μm within the bulk. Hence, as-received type A implants were already partially transformed at the surface. The bulk presented with average grain size of 0.35 μm and a dense microstructure with only a few micro-pores, which indicates efficient sintering of the bulk.

Type B implants presented with the smallest grain size (0.25 μm) compared to other types. Micro-pores were also present along the surface but were isolated with no interconnectivity. Surface micro-cracks extended an average depth of 0.5 μm . T-m transformations were also visible around micro-cracks and pores at the surface for average distance of 1.1 μm . The interior portions showed a dense microstructure without presence of cracks or pores.

Type C implants presented with average grain size of about 0.35 μm . Few micro pores and micro-cracks with depth of 0.3 μm were visible. Compared to the last two implants the as received type C implants presented with shallower (0.9 μm) and in most areas no evidence t-m transformation at the surface. The bulk of the material presented with few isolated porosities similar to type A.

Type D implants presented with average grain size of 0.35 μm . Surface presented with micro cracks, but no surface porosities, also consistent with surface SEM findings. Micro cracks ran along and parallel to the surface in a continuous pattern and extended from surface to bulk for average depth of 0.7 μm . Twining of grains were consistently visible along pre-existing micro-cracks and extended for an average depth of 1.8 μm within the bulk. Few pores were also visible within the bulk of the implant.

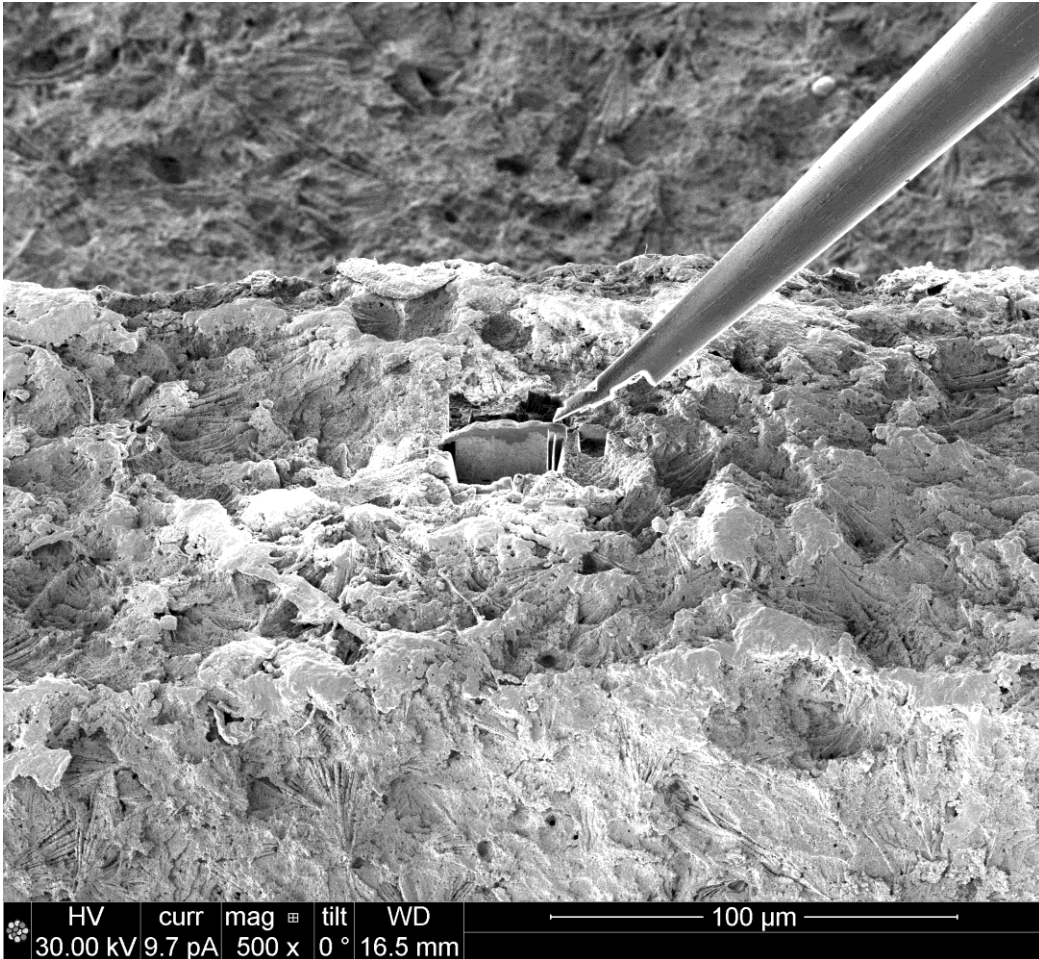
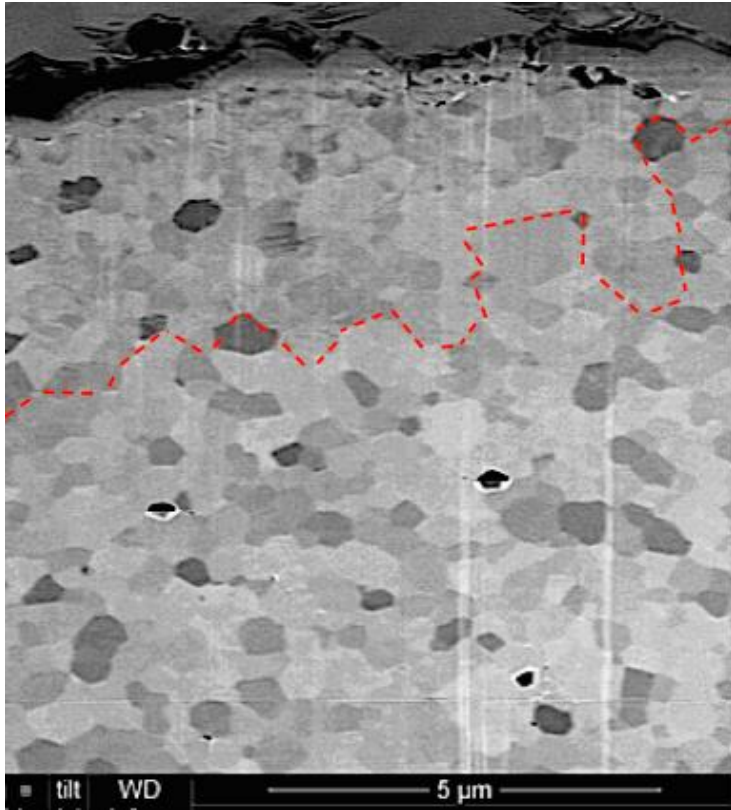
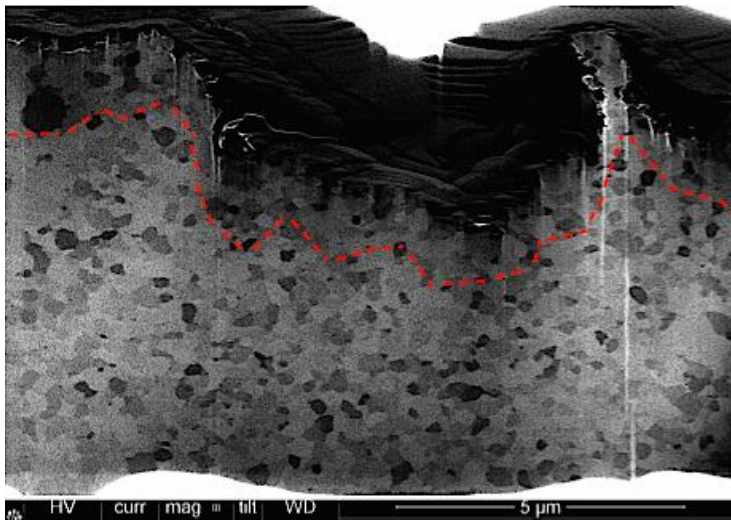


Figure 9. Low magnification of FIB image showing the location of ionic sectioning at the crest of the thread

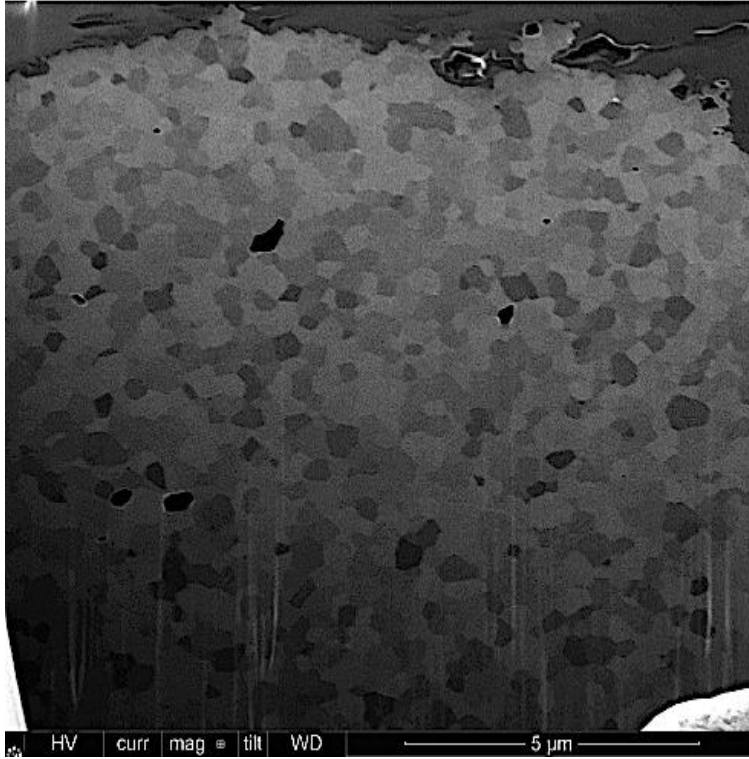


a) FIB cross section of type A implant

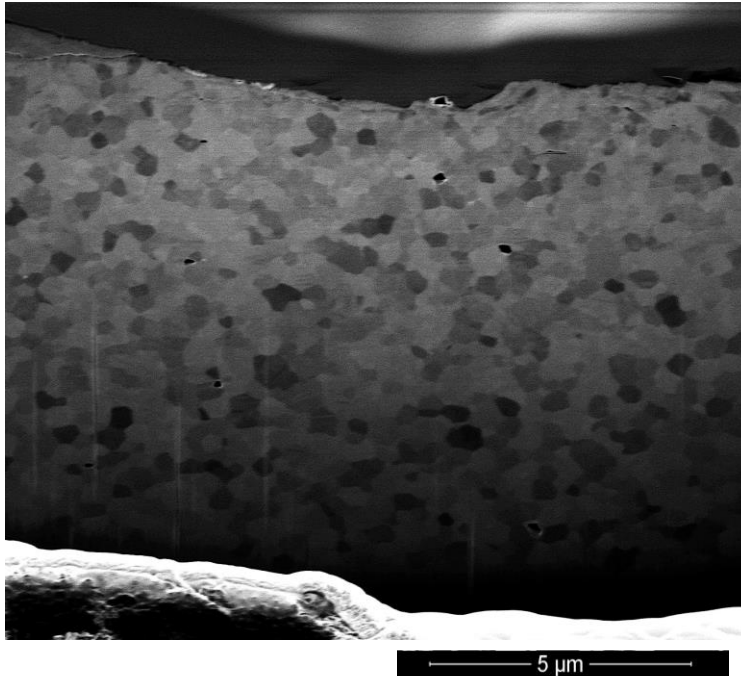


b) FIB cross section of Type B implant

Figure 10. High magnification of FIB cross section of as received implants



c) FIB cross section of type C implant



d) FIB cross section of type D implant

Figure 10. (Continued) High magnification of FIB cross section of as received implants

Microstructural Features of Aged Implants

Figure 4 provides the FIB cross-sections taken near the surface of 24 implants. Six implants were examined from each company, after an aging duration of 15 and 30 hours, with three implants with in each time interval.

Type A implants at 15 hours, presented with numerous nano scale porosities visible all along the surface. A higher number of micro-cracks were present parallel to each other and perpendicular to the surface and in some areas continuous with surface porosities. Within the bulk, the average depth of micro-cracks and t-m transformation slightly increased to 0.9 μm and 3.1 μm , respectively. At 30 hours, the microstructural changes as a result of aging became very clear. Surface porosities and micro-cracks increased in size and number respectively. Micro-cracks remained shallow (1 μm) and were continuous with micro-porosities. Zone of t-m transformation increased to a distance of 4.7 μm . Within this zone there were few grains that seemed to be unaffected and remained in their tetragonal phase. Overall, increased duration of aging led to greater quantity and dimension of surface cracks and porosities and consequently deeper penetration of transformed layer within the bulk. This result confirms previous findings [23] and illustrates that pre-existing porosities may have provided a pathway for water to penetrate within the bulk, which led to deeper layer of grain transformation at 15 hours. With longer aging time, deterioration of surface layer further facilitated the moisture entrance and led to higher extent of grain transformation.

Type B implants at 15 hours of aging presented with similar presentation to as received implants with shallow depths of micro-cracks (0.7 μm) and grain transformation (1.2 μm). At 30 hours, these features consistently remained superficial at depths of 0.6

μm and $1.5 \mu\text{m}$, respectively. Extent of micro-cracks and porosities seemed to be comparable to as received implants throughout different aging durations. From our observation, it appeared that hydrothermal aging did not have much influence on microstructural integrity of type B implants, despite presence of pre-existing micro-cracks and surface porosities.

Type C implants presented with micro-cracks remaining shallow at the surface with depth of $0.3 \mu\text{m}$ at 15 hours. The extent and depth of porosities and micro-cracks remained similar to as-received implants and the depth of t-m transformation slightly increased to $1.4 \mu\text{m}$. At 30 hours, number of micro-cracks clearly increased at the surface and its depth to an average distance of $1.5 \mu\text{m}$. The micro-cracks extended from the surface towards the bulk, following borders of the grains and appeared to be interconnected and continuous with micro-porosities. Depth of t-m transformation also increased to an average distance of $2.5 \mu\text{m}$. An important observation at 30 hours was the uplift of the surface and delamination of its portion, which is expected to happen as a result of aging. The results in this particular sample indicated that similar to type A, hydrothermal aging seemed to be gradual at 15 hours, but at 30 hours there was an obvious loss of structural integrity on the microstructure of the material.

Lastly, at 15 hours, micro-cracks remained superficial ($0.8 \mu\text{m}$) for type D implants and depth of t-m transformation slightly increased to $2.3 \mu\text{m}$. The pattern of micro-cracks at the surface was similar to as-received implants with long continuous cracks parallel to the surface with no porosities. At 30 hours the depth of micro-crack increased to average depth of $1.3 \mu\text{m}$ with increased number of isolated micro-cracks, followed by increased t-m transformation to a depth of $4.1 \mu\text{m}$. Pattern of grain

transformation seemed to be homogeneous with almost all grains appearing to be transformed with in the zone. The effect of LTD on microstructure of this group of implants was similar to type A and C.

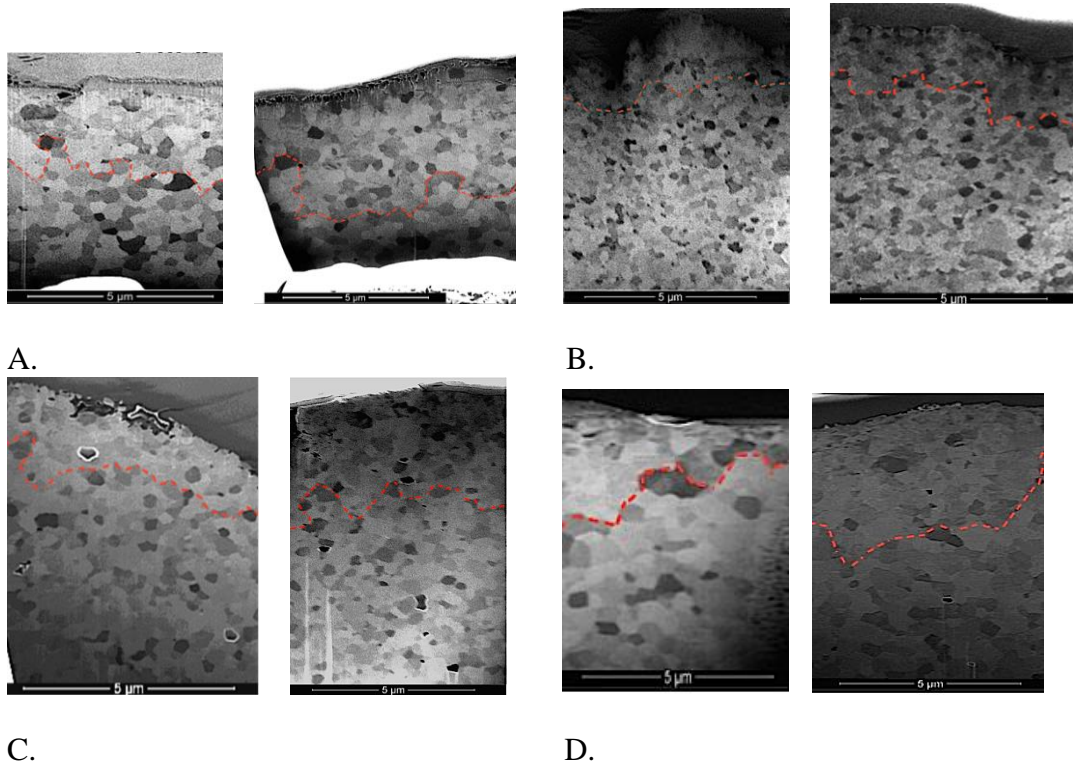


Figure 11. High magnifications of FIB cross sectional slices of aged implants at 15 and 30 hours. A: type A, B: type B, C: type C, D: type D

Statistical Results

Spearman's rho correlations among the measured variables for the entire sample (36 implants) showed significant correlation at $p \leq 0.01$. Increase in duration of aging was significantly and strongly correlated with increase in depth of t-m transformation in all aging durations (table 2). Nevertheless, no correlation was found in terms increased duration of aging and depth of micro-crack formation. We reject the null hypothesis that

there is no correlation between increasing period of aging and the depth of t-m transformation. Furthermore, we retain the null hypothesis that there is no correlation between increasing period of aging and depth of micro-crack formation.

Independent sample Kruskal-Wallis test showed no significant difference between groups in terms of depth of micro-crack formation at different duration of aging (Table. 3).

However, significant differences were found between groups with regards to depth of t-m transformation at different duration of hydrothermal aging ($p \leq 0.05$) as shown in table. 4.

We rejected the null hypothesis that there are no significant micro-structural differences between groups at 0 hour, 15 hours and 30 hours of aging.

Dunn-Bonferroni pair wise analysis showed significantly higher depth of t-m transformation in type A at zero hours compared to type C (Table. 5) . No significant differences were found among samples at 15 hours of aging, but at 30 hours, there was a significantly increased depth of t-m transformation in type A compared to type B ($p \leq 0.05$) as shown in table. 6. Presence of small sample size did not warrant further analysis with in each group.

Table 2. Spearman's rho correlation for entire sample of implants, between increase in aging duration and depth of t-m transformation and microcrack formation

T-M transformation		0 hours	15 hours	30 hours
0 hours	Rho	–	0.751^{**}	0.715^{**}
	N	12	12	12
15 hours	Rho	0.751^{**}	–	0.769^{**}
	N	12	12	12
30 hours	Rho	0.715^{**}	0.769^{**}	–
	N	12	12	12

****** $p \leq 0.01$

Table 3. Independent samples Kruskal-Wallis test among samples: microcrack formation

Null Hypothesis H ₀	Test	Sig.	Decision
Micro-crack at 0 hours is the same	Kruskal-Wallis test	0.507	Retain H ₀
Micro-crack 15 hours is the same	Kruskal-Wallis test	0.062	Retain H ₀
Micro-crack at 30 hours is same	Kruskal-Wallis test	0.104	Retain H ₀

***** $p \leq 0.05$

Table 4. Independent sample Kruskal-Wallis test among samples: t-m transformation

Null Hypothesis H_0	Test	Sig.	Decision
T-m transformation at 0 hours is the same	Kruskal-Wallis test	.015	Reject H_0 *
T-m transformation at 15 hours is the same	Kruskal-Wallis test	.043	Reject H_0 *
T-m transformation at 30 hours is the same	Kruskal-Wallis test	.021	Reject H_0 *

*
 $p \leq 0.05$

Table 5. Dunn-Bonferroni pairwise comparison after adjustment for multiple testing at 0 hours

Depth of t-m transformation (0 hours)	Test Statistic	Std. Error	Std. Test Statistic	Sig.	Adj. Sig
C-B	3.000	2.934	1.023	0.306	1.000
C-D	-6.000	2.934	-2.045	0.41	0.245
C-A	9.000	2.934	3.068	0.002	0.013*
B-D	-3.000	2.934	-1.023	0.306	1.000
B-A	6.000	2.934	2.045	0.041	0.245
D-A	3.000	2.934	1.023	0.306	1.000

* $p \leq 0.05$

Table 6. Dunn-Bonferroni pairwise after adjustment for multiple testing at 30 hours

Depth of t-m transformation (0 hours)	Test Statistic	Std. Error	Std. Test Statistic	Sig.	Adj. Sig
B-C	-3.000	2.939	-1.021	0.307	1.000
B-D	-5.500	2.939	-1.872	0.061	0.368
B-A	8.833	2.939	3.006	0.003	0.016*
C-D	-2.500	2.939	-0.851	0.395	1.000
C-A	5.833	2.939	1.985	0.047	0.283
D-A	3.333	2.939	1.134	0.257	1.000

* $p \leq 0.05$

CHAPTER 4

DISSCUSSION

The present set of data confirmed previous findings [35, 40], that FIB cross sectioning enabled a detailed characterization of zirconia implant's microstructure. Furthermore, it provided direct evidence of the effect of LTD on microstructure of the material as shown by extent of grain transformation, micro-cracks and microporosities. It also provided additional evidence to support previous data [43], that gentle preparation method by FIB milling did not induce t-m transformation due to mechanical stress, which was the main problem from previous approaches of mechanical cutting, grinding and polishing of samples for SEM analysis. This was apparent from FIB cross sectional images of as-received type C implants, which showed no evidence of t-m transformation in majority portion of their surfaces. However, FIB analysis was not without limitations. This process was very time-consuming (~6 hr/sample), technique sensitive and an expensive way to prepare cross sections. Consequently, we were restricted from having a large sample size, which was a weakness of our study. Having acknowledged that, the few available studies [35, 40, 43] with similar technique have completed FIB analysis on much smaller sample sizes due to limitations mentioned earlier. In addition, XRD analysis was not performed as it was reported earlier that due to reduced depth of x-ray penetration and the lack of precision of this type of analysis can give rise to under estimation of the result and generate misleading data [35, 40]. Furthermore, XRD analysis is not very precise for monoclinic contents lower than 5%, making it unsuitable for monitoring the beginning of transformation [19]. Moreover, it only gives an average monoclinic content over the penetration depth of the x-ray (which depends on the

density/porosity of the surface) and makes comparisons impossible on the pattern of transformation [35, 43]. Therefore, all the efforts were concentrated on FIB cross sectional images of implants to provide visual presentation of the effect of LTD on the microstructure of the material.

With regards to our result, FIB/SEM investigation revealed that after 15 hours of accelerated aging the effect of LTD on microstructure of all implants was minimal. Also, no significant differences were found among groups at 15 hours as it was illustrated by our pair-wise comparisons. At 30 hours, the effect of LTD became very clear for types A, C and D with increased surface porosities, microcracks, surface uplift, delamination and deep layer grain transformation. Accelerated aging however did not seem to effect the microstructure of type B implant at 30 hours. With regards to their pre-existing surface features, type B showed pre-existing microcracks, which seemed to be in higher amount compared to as-received type C. Type B also presented with surface porosities, which were absent in type D. While type B showed similar amount of surface porosities and microcracks to type A, it had a significantly shallower depth of t-m transformation at 30 hours compared to A. Previous reports have indicated that surface porosities and microcracks formed by surface roughening procedures, leads to reduction of surface density, which has been proposed to be the most important parameter in aging [6]. These open porosities and cracks offer water molecules easy access to the bulk, resulting in aging not only on the surface but also in the interior of the material [19, 40]. An earlier study with similar FIB analysis showed that the implant with a porous surface had a high number of transformed grains around the pores prior to accelerated aging, and that the porous surface increased the susceptibility of the implant to aging when it was compared

to another implant with polished dense surface [35]. We found similar results with regards to type A. However, one would expect type B to be similarly (compared to A) or even more extensively (compared to C and D) effected by accelerated aging. This was not the case in our results. This observation indicated that factors other than surface modification and density may have played an important role with regards to susceptibility of these implants to LTD.

In addition to density and surface treatment, other factors such as grain size and stabilizer's size, type and content have been indicated to effect susceptibility of zirconia ceramics to LTD [6, 44]. It has been widely accepted that reducing the grain size has a beneficial effect on stability of tetragonal phase and resistance to LTD [44]. However, decreasing the grain size may also reduce the stress induced transformation and lead to a decrease in fracture toughness, mainly because of less efficient phase transformation toughening [36, 44]. In our analysis Type B implants presented with smallest grains size averaging to about 0.25 μm compared to 0.35 μm for other implants. This property could be a contributing factor to its higher resistance to LTD at 30 hours.

With regards to chemical stabilizer, Y_2O_3 is the most widely used stabilizer and typically 3 mol % is used to stabilize the tetragonal phase to room temperature [44]. Increasing Y_2O_3 content improves resistance to LTD, but it can also inhibit the t-m transformation, thus decreasing the mechanical properties of the material [45]. Doping Y-TZP with other oxides specifically Ceria and Alumina (between 0.15% and 3%) has shown to provide satisfactory balance between aging resistance and mechanical properties [43, 22]. Chemical stabilizers, stress and grain size have been shown to be interlinked and to effect one another in a complex way. It is established that an increase in

content of stabilizer induces a reduction of the grain size while a larger grain size leads to higher local stress [44]. This may indicate that type B implants have a higher content of stabilizer, which has led to their smaller grain size and more resistance to aging. The larger grain sizes of other types could account for higher local stress and contribute to their susceptibility to aging. Nevertheless these are speculations, which can not be proven at this point, as we do not have information on specific concentration of stabilizers and other additives and it is beyond the effort of this study to evaluate this. However, our assessment provided some evidence that factors other than surface modification, such as the material's structural detail (grain size) and its composition (stabilizer, impurities, additives) may be more imperative than surface features for the increased resistance/susceptibility of zirconia ceramics to aging.

Finally, the present study was the first to provide visual data on the influence of LTD on microstructure of these commercially available zirconia implants. It also provided further evidence that T-M transformation starts from the surface and proceeds inwards with increasing number of microcracks, which opens the possibility for water to penetrate deeper triggering increased t-m transformation as shown in A,C and D.

CHAPTER 5

CONCLUSION

With in the limitations of this study we conclude that:

- FIB/SEM provided direct evidence of the transformation behavior for different zirconia dental implants following increasing aging durations.
- Aging showed a loss in structural integrity described by
 - Grain transformation evident by loss of grain boundaries and twinning between grains
 - Increased number of micro-porosities (A) and microcracks (A, C, D)
 - Surface uplift, grain pull out/delamination (C)
- LTD following accelerated aging minimally influenced the microstructure of implants at 15 hours, while at 30 hours, it had a more severe impact on types A, C and D compared to type B.
- The resistance to LTD could be more related to structural detail and composition of our currently investigated zirconia ceramics than the features of surface topography as a result of surface roughening procedures

Future research is needed to evaluate the effect of LTD on fatigue resistance of these implants. In addition, later invivo studies are needed to investigate the effect of mastication force on extent of LTD and the influence of surface changes such as delamination on surrounding hard and soft tissue.

REFERENCES

1. Piconi C, Maccauro G. Zirconia as a ceramic biomaterial. *Biomaterials* 1999; 20: 1–25.
2. Kisi E, Howard C. Crystal structures of zirconia phases and their interrelation. *Key Eng Mater* 1998;153/154:1-35
3. Garvie RC, Hannink RH, and Pascoe RT. Ceramic steel? *Nature* 1975; 258: 703-704.
4. Garvie RC, Nicholson PS. Phase analysis in zirconia systems. *J Am Ceram Soc* 1972;55:303-5
5. Passerini L. Isomorphism among oxides of different tetravalent metals: CeO₂–ThO₂; CeO₂–ZrO₂; CeO₂–HfO₂. *Gazzet Chim Ital* 1939;60:762–76.
6. Ruff O, Ebert F. Refractory ceramics: I. The forms of zirconium dioxide. *Z Anorg Allg Chem* 1929;180:19–41.
7. Fassina P, Zaghini N, Bukat A, Piconi C, Greco F, Piantelli S. Yttria and calcia partially stabilized zirconia for biomedical applications. *Bioceramics and the human body*. London and New York: Elsevier Applied Science; 1992. p. 223–9
8. Garvie RC, Urbani C, Kennedy DR, McNeuer JC. Biocompatibility of magnesia partially stabilized zirconia (mg-PSZ) ceramics. *J Mater Sci* 1984;19:3224–8.
9. Chevalier J, Deville S, Munch E, Jullian R, Lair F. Critical effect of cubic phase on aging in 3mol% yttria-stabilized zirconia ceramics for hip replacement prosthesis. *Biomaterials* 2004;25:5539–45.
10. Ban S, Sato H, Suehiro Y, Nakahishi H, Nawa M. Biaxial flexure strength and low temperature degradation of Ce-TZP/Al₂O₃ nanocomposite and Y-TZP as dental restoratives. *J Biomed Mater Res B: Appl Biomater* 2008;87B:492–8.
11. Denry I, Kelly JR. State of the art of zirconia for dental applications. *Dent Mater* 2008; 24:299-307.
12. Garvie RC, Hannink RH, and Pascoe RT. Ceramic steel? *Nature* 1975; 258: 703-704.
13. Gupta TK, Lange FF, Bechtold JH. Effect of stress-induced phase transformation on the properties of polycrystalline zirconia containing metastable tetragonal phase. *Journal of Materials Science* 1978; 13: 1464–1470.
14. Gupta TK, Bechtold JH, Kuznicki RC, Cadoff LH, Rossing BR. Stabilization of tetragonal phase in polycrystalline zirconia. *Journal of Materials Science* 1977;

- 12: 2421–2426.
15. Kobayashi K, Kuwajima H, Masaki T. Phase change and mechanical properties of ZrO₂-Y₂O₃ solid electrolyte after ageing. *Solid State Ionics* 1981; 3:489–493.
 16. Chevalier J. What future for zirconia as a biomaterial? *Biomaterials* 2006; 27:535-543
 17. Li J, Watanabe R. X-ray photoelectron spectroscopy investigation on the low-temperature degradation of 2 mol % ZrO₂-Y₂O₃ ceramics. *J Am Ceram Soc* 1996; 79:3109-12.
 18. Lee JK, Kim H. Surface crack initiation in 2Y-TZP ceramics by low temperature aging. *Ceram Int* 1994;20:413-8.
 19. Chevalier J, Gremillard L, Deville S. Low-temperature degradation of zirconia and implications for biomedical implants. *Annu. Rev. J Mater Res* 2007; 37:1–32.
 20. Yoshimura M, Noma T, Kawabata K, Somiya S. Role of H₂O on degradation process of Y-TZP. *J Mater Sci Lett* 1987; 6:465-467.
 21. Lawson S. Environmental degradation of zirconia ceramics. *J Eur Ceram Soc* 1995:485-502
 22. Chevalier J, Gremillard L, Virkar AV, Clarke DR. The tetragonal-monoclinic transformation in zirconia: lessons learned and future trends. *J Am Ceram soc* 2009; 92:1901-1920.
 23. Yoshimura M. Phase-stability of zirconia. *Am Ceram Soc Bull* 67: 1950-1955.
 24. Christel PS. Zirconia: the second generation of ceramics for total hip replacement. *Bulletin of the Hospital for Joint Diseases Orthopaedic Institute* 1988; 49: 170–177.
 25. Clarke IC, Manaka M, Green DD, William P, Pezzotti G, Kim YH. Current status of zirconia used in total hip implants 2003. *J Bone Joint Surg Am* 85-A Suppl 4:73-84
 26. Ozkurt Z, Kazazoglu E. Zirconia dental implants: a literature review. *Journal of Oral Implantology* 2011; 37: 367–376.
 27. Chevalier J, Loh J, Gremillard L, Meille S, Adolfson E. Low-temperature degradation in zirconia with a porous surface. *Acta Biomaterialia* 2011; 7:2986–2993.

28. Kohorst P, Herzog TJ, Borchers L, Stiesch-Scholz M. Load-bearing capacity of all-ceramic posterior four-unit fixed partial dentures with different zirconia frameworks. *European Journal of Oral Sciences* 2007; 115: 161–166.
29. Wenz HJ, Bartsch J, Wolfart S, Kern M. Osseointegration and clinical success of zirconia dental implants: a systematic review. *The International Journal of Prosthodontics* 2007; 21: 27–36.
30. Manicone P, Rossi Iommetti P, Raffaelli L. An overview of zirconia ceramics: basic properties and clinical applications. *Journal of Dentistry* 2007;35:819–26.
31. Studart A, Filser F, Kocher P, Gauckler L. Fatigue of zirconia under cyclic loading in water and its implications for the design of dental bridges. *Dent Materials* 2007; 23:106-14
32. Yamashita D, Machigashira M, Miyamoto M, Takeuchi H, Noguchi K, Izumi Y, et al. Effect of surface roughness on initial responses of osteoblast-like cells on two types of zirconia. *Dental Materials Journal* 2009; 28: 461-70
33. Alghazzawi TF, Lemons J, Liu PR, Essig ME, Bartolucci AA, Janowski GM. Influence of low-temperature environmental exposure on the mechanical properties and structural stability of dental zirconia. *Journal of Prosthodontics* 2012; 21: 363–369.
34. Kohorst P, Borchers L, Stempel J, Stiesch M, Hassel T, Bach FW, Hubsch C. Low-temperature degradation of different zirconia ceramics for dental applications. *Acta Biomaterialia* 2012; 8:1213– 1220.
35. Sanon C, Chevalier J, Douillard T, Kohal RJ, Coelho PG, Hjerpe J, Silva N. Low temperature degradation and reliability of one-piece ceramic oral implants with a porous surface. *Dental Materials* 2013; 29: 389–397.
36. Cattani-Lorente M, Scherrer SS, Ammann P, Jobin M, Wiskott HW. Low temperature degradation of a y-tzp dental ceramic. *Acta Biomaterialia* 2011; 7:858–865.
37. Flinn BD, Degroot DA, Mancl LA, Raigrodski AJ. Accelerated aging characteristics of three yttria-stabilized tetragonal zirconia polycrystalline dental materials. *The Journal of Prosthetic Dentistry* 2012;108:223–230.
38. Borchers L, Stiesch M, Bach FW, Buhl JC, Hubsch C, Kellner T, Kohorst P, Jendras M. Influence of hydrothermal and mechanical conditions on the strength of zirconia. *Acta Biomaterialia* 2010; 6:4547–4552.

39. Marro FG, Anglada M. Strengthening of vickers indented 3Y-TZP by hydrothermal ageing. *Journal of the European Ceramic Society* 2012; 32 :317–324.
40. Sanon C, Chevalier J, Douillard T, Cattani-Lorente M, Scherrer SS, Gremillard L. A new testing protocol for zirconia dental implants. *Dental Materials* 2015; 31:15–25.
41. Oliva X, Oliva J, Oliva J, Prasad HS, Rohrer MD. Osseointegration of Zirconia Y-TZP dental implants: a histologic, histomorphometric and removal torque study in the hip of sheep. *Int J Implantol Clin Res* 2013; 4(2):00-00.
42. Chappuis V, Cavusoglu Y, Gruber R, Kuchler U, Buser D, Bosshardt DD. Osseointegration of Zirconia in the Presence of Multinucleated Giant Cells. *Clinical implant dentistry and related research*. 2015.
43. Keuper M, Eder K, Berthold C, Nickel KG. Direct evidence for continuous linear kinetics in the low-temperature degradation of Y-TZP. *Acta biomaterialia*. 2013; 9(1):4826-35.
44. Lughì V, Sergo V. Low temperature degradation-aging-of zirconia : A critical review of the relevant aspects in dentistry. *Dental materials*. 2010 Aug 31; 26(8):807-20
45. Tsubakino H, Nozato R, Hamamoto M. Effect of alumina addition on the tetragonal to monoclinic phase transformation in zirconia-3 mol% yttria. *J. Am. Ceram. Soc.* 1991; 74: 440-43